地震研究所彙報
Bull. Earthq. Res. Inst.
Univ. Tokyo
Vol. 78 (2003) pp. 59-65

Fracture surface energy of natural earthquakes from the viewpoint of seismic observations

Satoshi Ide*

Department of Earth and Planetary Science, University of Tokyo

Abstract

Fracture surface energy, G_c, is one of the fundamental parameters that governs earthquake rupture propagation and seismic energy radiation. Unlike other parameters of friction, it is relatively easily estimated using seismic observations. In this paper we consider two aspects of G_c, 1) the implications of the minimum G_c for the scaling of seismic energy, and 2) spatial distribution of G_c calculated from kinematic source models. Analyses of G_c based on seismic observations are important when comparing in-situ and laboratory observations of fault materials, which will be obtained in the Nankai-drilling project.

Key words: fracture surface energy, G_c, earthquake scaling, energy budget

1. Introduction

The earthquake source process includes rupture propagation, which consumes energy to create new fracture surfaces. Although an earthquake source is also regarded as slippage of preexisting weak planes, the strength of such planes may be recovered by a healing process during an interseismic period in the geological scale, and a considerable amount of energy is required for them to slip again. This energy is called fracture surface energy and is written as G_c. If we consider G_c as a material property such as free surface energy or fracture energy of tensile fracture, this must be a constant and total fracture surface energy of an earthquake scales with the fault area as 2D quantity. Potential energy release and seismic energy by earthquake scale with seismic moment and are 3D quantities. This leads to the conclusion that for a large earthquake, the fracture surface energy of 2D is negligible compared to 3D potential energy release and seismic energy (e.g., Kostrov, 1974).

However, G_c cannot be considered to be a material property because we cannot distinguish the energy consumption required to create a main fault plane among the various kinds of energy consumption, such as microcracking, plastic deformation, and abrasion within the fault zone. Frictional work by the slip component whose direction is perpendicular to the main slip vector should be included in the fracture energy. Inelastic attenuation of seismic waves near the fault zone is also indistinguishable from other forms of energy consumption. Intuitively, the width of the zone where such a physical processes take place increases as event size increases. This is also consistent with the fact that the width of microcracking zone scales with fault length from field observations (Vermilye and Scholz, 1998). Therefore, G_c scales not only with fault area but also with another dimension such as fault zone width. Thus, G_c is considered to be a 3D property, although we call it fracture surface energy. It is not obvious whether or not this is negligible compared to seismic energy for natural earthquakes.

G_c scales with event size in laboratory experiments (Ohnaka, 2003) and field observations (Scholz, 2002). There have been attempts to measure the G_c of the overall rupture process of large earthquakes (e.g., Husseini, 1975; Papageorgiou and Aki, 1983), and these values, 10^{4-8} J/m^2, are usually much higher than those obtained in a laboratory experiment. G_c can be estimated locally based on rupture models of large events (Beroza and Spudich, 1988; Guatteri *et al.*, 2001), and its maximum is about 10^6 J/m^2 for M7 class earthquakes.

* e-mail: ide@eps.s.u-tokyo.ac.jp (7-3-1, Hongo, Bunkyo, Tokyo, 113-0033, Japan)

In this paper we discuss two aspects of the surface fracture energy of natural earthquakes. First, based on recent studies of seismic energy scaling (Ide and Beroza, 2001; Ide *et al.,* 2003), we consider what we expect in the presence of the minimum value of G_c. Second, we estimate the spatial distribution of G_c for an earthquake, the 1995 Kobe earthquake of M_w 6.8, based on a study of the energy balance using a kinematic model (Ide, 2002). We also briefly discuss the relation with possible outcomes from the Nankai drilling project.

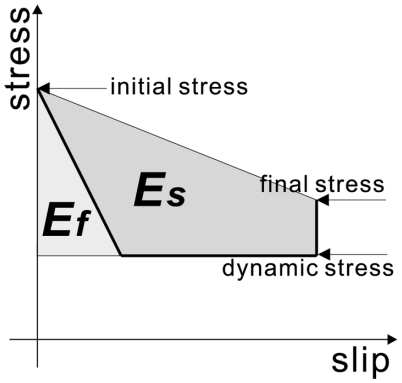

Fig. 1. Stress and stress relation during faulting process and energy balance. Shaded areas represent the amount of seismic energy (E_s) and fracture energy (E_F). E_F is given by the integral of G_c over the fault plane as defined by equation (1).

2. Minimum event and G_c

As illustrated in Fig. 1, the potential energy released by an earthquake is divided into two parts, seismically radiated energy (seismic energy) E_s, and unradiated energy consumption (fracture energy) E_f, which is the G_c integrated across fault area Σ,

$$E_f = \int_{\Sigma} G_c dS. \qquad (1)$$

Many studies have estimated seismic energy, E_s, for earthquakes of various sizes, showing the size dependences of energy and moment ratio, E_s/M_o, or apparent stress, $\sigma_a = \mu E_s/M_o$, where μ is the rigidity of the source region (e.g., Abercrombie, 1995; Kanamori and Brodsky, 2001). However, it is still an open question whether or not apparent stress depends on earthquake size, and all previous estimates have presented little evidence of a breakdown of constant apparent stress scaling (Ide and Beroza, 2001). Fig. 2 is a summary of the apparent stress estimation. In the study of small events by Gibowicz *et al.* (1991) and Jost (1998), the energies seem to be substantially underestimated due to the band limitation, and we show the values after adding the energy that is probably missing as described in Ide and Beroza (2001). For events between M_w 0.5 and 3, we include recent studies using empirical Green's function method for Long Valley, California, (Ide *et al.,* 2003)

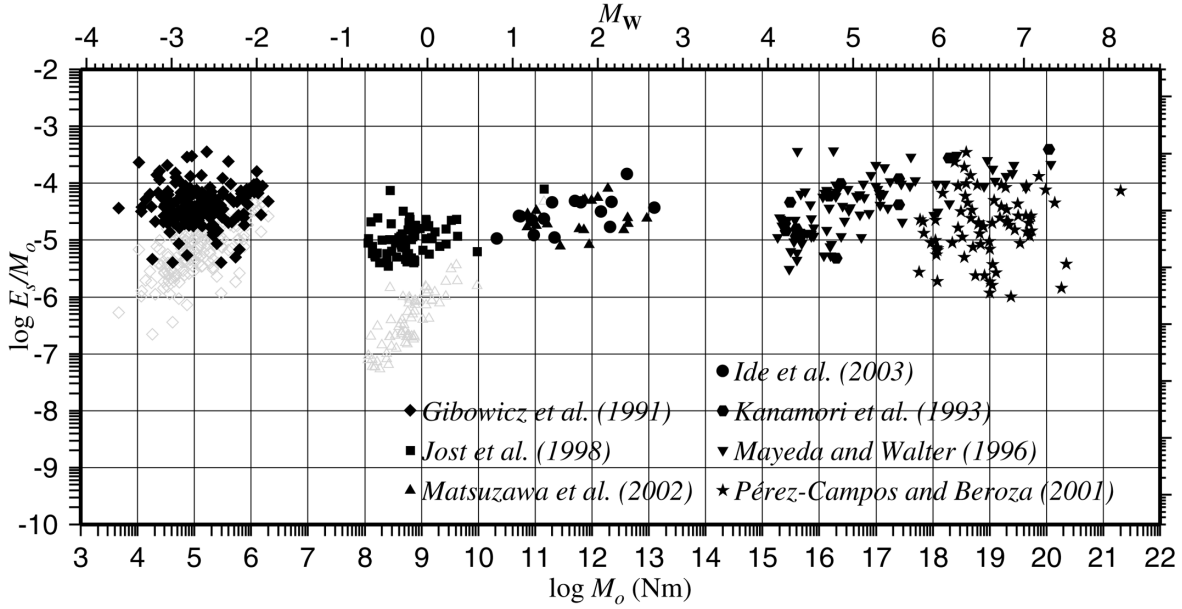

Fig. 2. Summary of studies of seismic energy. For small events of Gibowicz *et al.* (1991) and Jost *et al.* (1998), gray symbols are the values in the original papers and black symbols are those after adding potentially missing energy described by Ide and Beroza (2001).

and western Nagano, Japan, (Matsuzawa *et al.,* 2002). For the studies of intermediate and large earthquakes by Mayeda and Walter (1996) and Kanamori *et al.* (1993), we limit the minimum event size to M_w 4 to avoid an event selection bias as suggested by Ide and Beroza (2001).

All estimates of energy/moment ratio in Fig. 2 are located between 10^{-6} and 10^{-3}. Although it is not apparent in Fig. 2, there should be a breakdown of such constant energy/moment ratio scaling because fault motion consumes fracture surface energy, G_c, to create slipping surfaces. The energy can be quite small and may scale with event size as described later, but cannot be zero. For example, G_c is about 0.5 J/m^2 in a frictional slip experiment between two granite rocks of 30 cm (Ohnaka and Yamashita, 1989). Because earthquakes occur on an interface which has healed for a long time and is stronger than in such frictional experiments, it is difficult to imagine that the G_c of a natural fault is smaller than this value. For a mode I fracture, G_c is estimated to be 1–100 J/m^2 (Atkinson, 1984) and for a triaxial mode III fracture, G_c is on the order of 10^4 J/m^2 (Wong, 1982). The minimum is comparable to or less than these values, and the existence of the minimum suggests a breakdown of scaling.

To see the effects of the minimum fracture surface energy, consider a simple circular crack with a constant stress drop $\Delta\sigma$ and a radius of r_0. The average slip of this crack is

$$\overline{u}=\frac{16}{7\pi}\frac{\Delta\sigma}{\mu}r_0, \tag{2}$$

where μ is the rigidity. It is also represented using the seismic moment $M_o=\mu\pi r_0^2\overline{u}$ as,

$$\overline{u}=\left(\frac{256}{49}\right)^{1/3}\frac{1}{\pi\mu}\Delta\sigma^{2/3}M_o^{1/3}$$

$$\approx\frac{0.55}{\mu}\Delta\sigma^{2/3}M_o^{1/3}. \tag{3}$$

The summation of E_f and E_s is given from Fig. 1 as,

$$E_f+E_s=\frac{\Delta\sigma}{2\mu}M_o \tag{4}$$

which corresponds to the potential energy release minus frictional work for all fault area. If we take energy/moment ratio,

$$\frac{E_s}{M_o}=\frac{\Delta\sigma}{2\mu}-\frac{\int G_c dS}{M_o}$$

$$\approx\frac{\Delta\sigma}{2\mu}-\frac{\overline{G}_c}{0.55M_o^{1/3}\Delta\sigma^{2/3}}, \tag{5}$$

where $\overline{G}_c$ is the average G_c over the crack. This relationship of energy/moment ratio and seismic moment defines the minimum seismic moment for given $\overline{G}_c$ and $\Delta\sigma$.

Although $\overline{G}_c$ may scale with event size, we now consider only the minimum of $\overline{G}_c$, $G_c^{\min}$ for simplicity. Fig. 3 shows the relations between E_s/M_o and M_o for some combinations of $G_c^{\min}$ and $\Delta\sigma$ in equation (5). For example, $G_c^{\min}=100$ J/m^2 and $\Delta\sigma=0.1$ MPa predict that there are no earthquakes smaller than M_w 0. From observations of microearthquakes, this is a reasonable lower limit, but there are certainly many smaller events, for example, in mines. This fact implies that $G_c^{\min}$ is much smaller or $\Delta\sigma$ is much higher for such events. From observation of recurrence intervals of repeated earthquakes, Nadeau and Johnson (1998) calculated the stress drop for M2 earthquakes to be 270 MPa. Seno (2003) also estimated a high stress drop for small events based on his fractal asperity model. Such a large stress drop can explain the existence of small events, without assuming quite small fracture surface energy.

For real earthquakes, it is difficult to determine the static stress drop. It should be noted that stress drops determined by corner frequencies such as the Brune stress drop (Brune, 1970, 1971) are just alternative measures of seismic energy, and the static stress drop should be measured from other information such as aftershock distribution or stopping phases (Imanishi and Takeo, 2002). Once the information on stress drop is available and we can define the minimum event size within the event detection limit, we can estimate the value $G_c^{\min}$ for the region. For this purpose, high-sensitivity and high-sampling seismometers in deep boreholes with low noise play an important role. In particular, earthquake observations at boreholes of great depths in the Nankai subduction zone will provide us with an opportunity to estimate $G_c^{\min}$ along the subducting plate interface.

3. Spatial distribution of G_c on fault planes

Energy balance on a fault plane during an earthquake is expressed using local slip and stress relations (Kostrov, 1974). Using these relations and the finite difference method, Ide (2002) determined the spatial distribution of seismic energy for kinematic

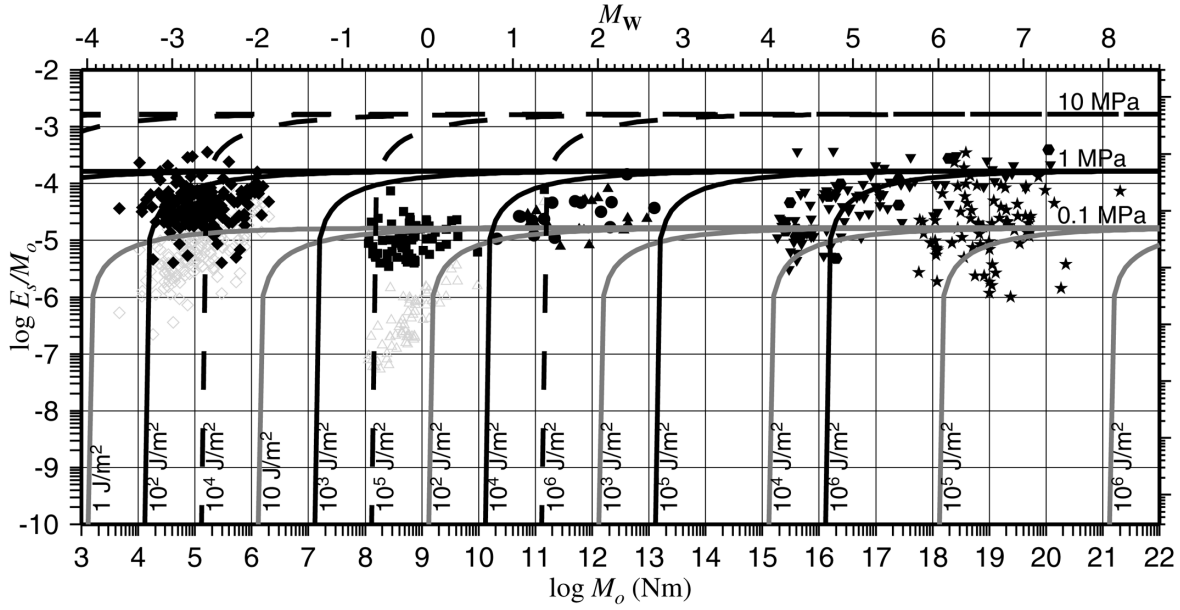

Fig. 3. The relation between the seismic energy/moment ratio and seismic moment predicted from the stress drop and the minimum fracture surface energy $G_c^{\min}$, superimposed on Fig. 2. Dashed, solid, and gray lines represent the stress drop of 10, 1, and 0.1 MPa, respectively. Assumed $G_c^{\min}$ is shown for each line.

source models of the 1995 Kobe, Japan, earthquake. It is also possible to calculate fracture surface energy, as well as seismic energy. However, the estimation of fracture energy is not as straightforward as that of seismic energy, because we need to define dynamic stress level.

Fig. 4 shows distributions of seismic energy density and fracture surface energy, and slip-stress relations at different points on the fault plane for the 1995 Kobe earthquake. It is not clear what the dynamic stress level is in each relation. In the present calculation, we assume dynamic stress level to be the minimum stress value in each slip-stress relation, which corresponds to the light gray area in the slip-stress relation in Fig. 4.

Such a calculation includes the contribution from artificial slip-weakening distance due to insufficient resolution (Ide and Takeo, 1997). In the finite difference calculation of inplane shear crack, stress, τ, just after initiation of slip, u, is approximated by,

$$\tau = -\mu \frac{u}{\Delta x}, \tag{6}$$

where Δx represents grid interval. Artificial fracture surface energy, G_c^a, is the product of artificial slip-weakening distance and stress drop divided by 2:

$$G_c^a = \frac{\tau^2 \Delta x}{2\mu}.$$

If the stress drop is 10 MPa, which is the maximum in this calculation, G_c^a is about 5×10^5 J/m^2. Because there is a broad area of G_c that is larger than 10^6 J/m^2, it cannot be explained merely by an artifact, and such a large fracture surface energy is essential to explain the rupture propagation behavior of the Kobe earthquake.

Fig. 4 shows areas of large G_c near the hypocenter (A) and shallow region around C. Theoretically, the hypocenter is a point where the surface fracture energy consumed after the hypocentral time is zero. However, if we use a grid system, G_c is averaged with the neighboring grids and we cannot obtain zero fracture energy, and there are artifacts as described, too. Therefore, the high G_c around the hypocenter is the combined result of the artifact and the averaging effect. Rather, a broad area with a large G_c to the northeast of the hypocenter is important. This area is necessary to decelerate northeastward rupture propagation at the initial stage of this earthquake. The area of high G_c around C corresponds to the Akashi strait, where the rupture process is separated into northeast and southwest. The surface traces of active faults are also discontinuous. Such a geographical irregularity may be responsible for the

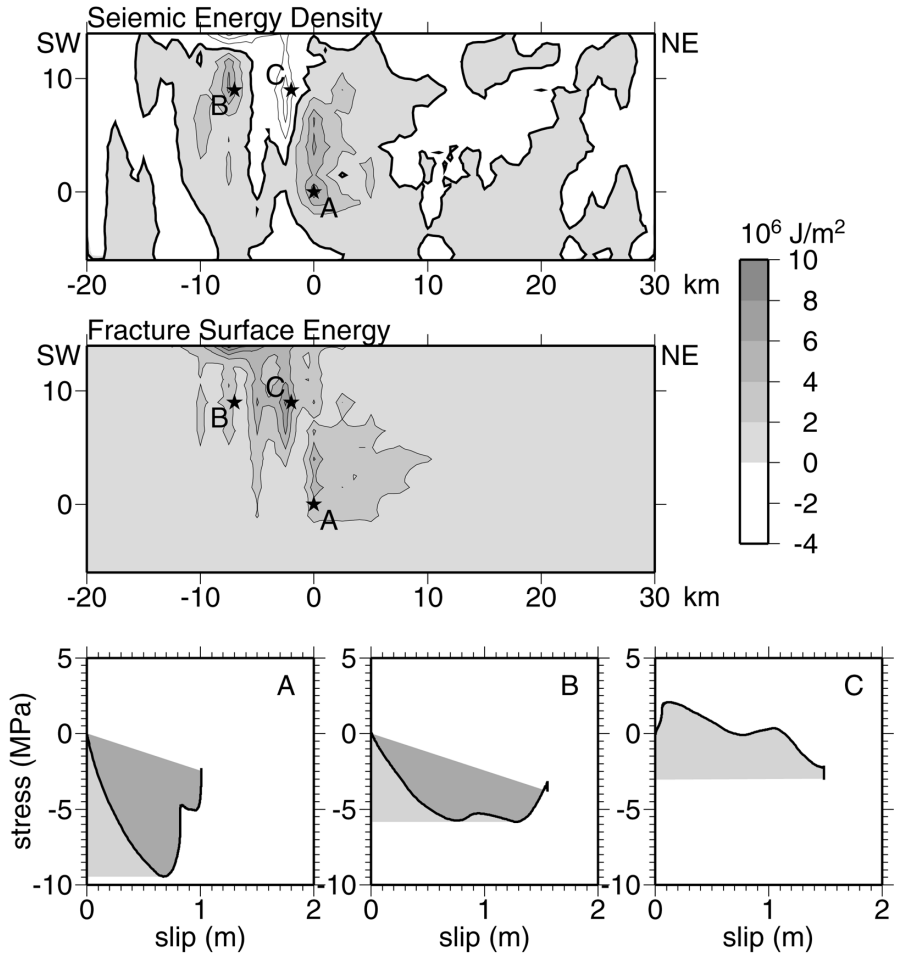

Fig. 4. Distribution of seismic energy density and fracture surface energy. Relations between slip and stress for three selected points are shown at the bottom. In each slip-stress relation, the dark gray area corresponds to seismic energy and the light gray area corresponds to fracture surface energy estimated in this paper.

high fracture surface energy.

The distribution of G_c in Fig. 4 is quantitatively consistent with the estimation using rate and state friction law (Guatteri *et al.,* 2001). The large G_c is also suggested by a dynamic simulation of the 1992 Landers earthquake of M_w 7.3 (Olsen *et al.,* 1997; Peyat *et al.,* 2002). They used the slip weakening friction law with a slip-weakening distance of 80 cm (Olsen *et al.,* 1997). Since the stress drop is on the order of 10 MPa, G_c is on the order of 10^7 J/m^2. The values of seismic energy density in these studies are almost of the same order as the fracture energy, so we cannot neglect G_c in the discussion of earthquake dynamics.

4. Discussion and Conclusion

Fracture energy represents energy consumption from real physical processes, such as production of microcracks, plastic deformation and abrasion. In the Nankai drilling project, we plan to drill through a megathrust fault to 5 km or deeper depth. In-situ observations of density, porosity, and microcrack density of the fault zone will be useful to distinguish which process is dominant in subduction earthquakes and may enable the estimation of G_c based on these observable quantities.

Although recent improvements in observation systems have been remarkable, it is still difficult to obtain sufficient data to determine details of slip history for future Tonankai or Nankai earthquakes. In such cases, the parameter estimated is fracture surface energy rather than other dynamic parameters such as breakdown stress and characteristic displacement of slip-weakening friction law (Guatteri and Spudich, 2000; Ide 2002). Using the method discussed in this paper, it is possible to measure the spatial distribution of large future events. Moreover,

if the size of the minimum event is well-defined, we can estimate the overall G_c of this area. An independent estimate of G_c from in-situ observation is useful for calibration, although we should be careful about the difference of scale.

Information about frictional properties, a and b of rate-and state-friction law, or breakdown stress drop and critical displacement of slip-weakening friction law, is critical to determine rupture propagation behavior. Experiments using rock samples from the actual fault zone are informative, but these are properties of almost one point on a large fault surface, and overall slip behavior may be irrelevant from these properties. On the other hand, what we can estimate from seismic waves are spatially averaged properties. The seismic observations and in-situ measurement in the Nankai trough will provide a good opportunity to obtain the values of both small and large scales, and consider scaling between them.

5. Acknowledgements

I thank Dr. Shingo Yoshida for suggesting errors in the manuscript. Figures are prepared using Generic Mapping Tool. This work is supported by Grant-in-Aid for Scientific Research of the Ministry of Education, Sports, Science and Technology and Special Project for Earthquake Disaster Mitigation in urban areas.

thebibliography

Abercrombie, R.E., 1995, Earthquake source scaling relationships from-1 to 5 using seismograms recorded at 2.5-km depth, *J. Geophys. Res.,* **100**, **24**, 01–24, 036.

Atkinson, B.K., 1984, Subcritical crack growth in geological materials, *J. Geophys. Res.,* **89**, 4077–4114.

Beroza, G.C. and P. Spudich, 1988, Linearized inversion for fault rupture behavior: application to the 1984 Morgan Hill, California earthquake, *J. Geophys. Res.,* **93**, 6275–6296.

Brune, J.N., 1970, Tectonic stress and spectra of seismic shear waves from earthquakes, *J. Geophys. Res.,* **75**, 4997–5009, 1970. (Correction, 1971, *J. Geophys. Res.,* **76**, 5002.)

Gibowicz, S.J., R.P. Young, S. Talebi, and D.J. Rawlence, 1991, Source parameters of seismic events at the Underground Research Laboratory in Manitoba, Canada: Scaling relations for events with moment magnitude smaller than-2, *Bull. Seismol. Soc. Am.,* **81**, 1157–1182.

Guatteri, M., and P. Spudich, 2000, What can strong motion data tell us about slip-weakening fault friction laws?, *Bull. Seism. Soc. Am.,* **90**, 98–116.

Guatteri, M., P. Spudich, and G.C. Beroza, 2001, Inferring rate and state friction parameters from a rupture models of the 1995 Hyogo-ken Nanbu (Kobe) earthquake, *J. Geophys. Res.,* **106**, 26511–26522.

Husseini, M.I., D B. Jovanovich, M.J. Randall, and L.B. Freund, 1975, The fracture energy of earthquakes, *Geophys. J. R. Astron. Soc.,* **43**, 367–385.

Kanamori, H. and E.E. Brodsky, 2001, The Physics of Earthquakes, *Physics Today,* **54**, 34–40.

Kanamori, H., E. Hauksson, L.K. Hutton, and L.M. Jones, 1993, Determination of earthquake energy release and using TERRAscope, *Bull. Seismol. Soc. Am.,* **83**, 330–346.

Kostrov, B.V., 1974, Seismic moment and energy of earthquakes and seismic flow of rock, *Izv. Earth Phys.,* **1**, 23–40.

Ide, S., 2002, Estimation of radiated energy of finite-source earthquake models, *submitted to Bull. of Seismol. Soc. Am.,* in press.

Ide, S., and G.C. Beroza, 2001, Does apparent stress vary with earthquake size? *Geophys. Res. Lett.,* **28**, 3349–3352.

Ide, S., G.C. Beroza, S.G. Prejean and W.L. Ellsworth, 2003, Apparent Break in Earthquake Scaling Due to Path and Site Effects on Deep Borehole Recordings, *J. Geophys. Res,* in press.

Ide, S., and M. Takeo, 1997, Determination of constitutive relations of fault slip based on seismic wave analysis, *J. Geophys. Res.,* **102**, 27379–27391.

Imanishi, M., and M. Takeo, 2002, An inversion method to analyze rupture processes of small earthquakes using stopping phases, *J. Geophys. Res.,* **107**, 10.1029/2001JB 000201.

Jost, M.L., T. Buselberg, O. Jost, and H.-P. Harjes, 1998, Source parameters of injection-induced microearthquakes at 9 km depth at the KTB deep drilling site, Germany, *Bull. Seismol. Soc. Am.,* **88**, 815–832.

Matsuzawa, T., M. Takeo, K. Imanishi, H. Ito, S. Ide, Y. Iio, S. Sekiguchi, S. Horiuchi, S. Ohmi, 2002, A scaling relationship of the seismic wave energies of the microearthquakes with the correction based on ω2-model, abs. SSJ, Yokohama, Japan, P 114.

Mayeda, K., and W.R. Walter, 1996, Moment, energy, stress drop, and source spectra of western United States earthquakes from regional coda envelopes, *J. Geophys. Res.,* **101**, 11,195–11208.

Nadeau, R.M. and L.R. Johnson, 1998, Seismological Studies at Parkfield VI: Moment Release Rates and Estimates of Source Parameters for Small Repeating Earthquakes, *Bull. Seism. Soc. Am.,* **88**, 790–814.

Ohnaka, M., 2003, A constitutive scaling law and a unified comprehension for frictional slip failure, shear fracture of intact rock, and earthquake rupture, *J. Geophys. Res.,* in press.

Ohnaka, M. and T. Yamashita, 1989, A cohesive zone model for dynamic shear faulting based on experimentally inferred constitutive relation and strong motion source parameters, *J. Geophys. Res.,* **94**, 4089–4104.

Olsen, K.B., R. Madariaga, and R.J. Archuleta, 1997, Three-dimensional dynamic simulation of the 1992 Landers earthquake, *Science* **278**, 834–838.

Papageorgiou, A.S., and K. Aki, 1983, A specific barrier model for the quantitative description of inhomogeneous faulting and the prediction of strong ground motion, II. applications of the model, *Bull. Seism. Soc. Am.,*

73, 953–978.

Peyrat, S., K. B. Olsen, R. Madariaga, 2001, Dynamic modeling of the 1992 Landers earthquake, *Jour. Geophys. Res.* **106**, 26,467–26,482.

Scholz, C. H.,, 2002, The mechanics of earthquake and faulting-2nd ed., Cambridge University Press, Cambridge, UK.

Seno, T., 2003, Fractal asperities, invasion of barriers,and interplate earthquakes, *J. Geophys. Res.*, submitted.

Vermilye, J. M., and C. H. Scholz, 1998, The process zone: a microstructural view of faulting, *J. Geophys. Res.* **103**, 12223–12237.

Wong, T.-F., 1982, Shear fracture energy of Westerly granite from post-failurebehavior, *J. Geophys. Res.*, **87**, 990–1000.

(Received February 3, 2003)
(Accepted April 25, 2003)